International Research Journal of Multidisciplinary Scope (IRJMS), 2024; 5(1):62-73 IRJMS

Original Article | ISSN (O): 2582-631X DOI: 10.47857/irjms.2024.v05i01.0145

Real Time Object Detection in Low Light Environment Using Adaptive Image Information Enhancement Algorithm

Madhan K, Shanmugapriya N*

Department of CSE, Dhanalakshmi Srinivasan University, Samayapuram, Trichy, Tamil Nadu, India. *Corresponding Author's Email: shanmugapriyan.set@dsuniversity.ac.in

Abstract

Object detection plays a vital role in CCTV systems. Cameras are now deployed at traffic lights, roadways, shopping centers, railways, banks, and other public locations to increase security. It isn't easy to follow the video quickly and continuously, though. Therefore, surveillance cameras are not required, and human surveillance is needed. A significant difficulty for CCTV cameras is detecting anomalies such as theft, accidents, crimes, and other illegal activities. The frequency of abnormal behaviour is the same as that of regular events. To detect objects in a video, we first analyze each pixel in the image. Segmentation in digital photography is the process of dividing different parts of an image into pixels. Segmentation performance is affected by uneven and dim lighting. These factors significantly impact the real-time object detection process of CCTV systems. In this article, we propose an Adaptive Image Information Enhancement Algorithm (AIIE) to improve images affected by poor lighting. Test results compare the output of the current method with the improved ResNet model architecture and show significant improvement in object detection in video streams. The proposed model delivers better results regarding metrics such as precision, recall, and pixel precision. We also saw significant improvements in object detection.

Keywords: AIIE, object quality, Low Light, Object Detection, Resnet.

Introduction

Image processing in low-light conditions poses significant challenges, often resulting in reduced image quality due to inadequate illumination. The distortion in image information can severely impact critical image processing applications such as object detection and surveillance. Real-time object detection is crucial in video surveillance systems, automatically detecting anomalies or unusual events (1). However, the performance of such systems is hindered by the vast data volume in video streams, demanding high-quality images for effective object detection. In dynamic environments, especially during nighttime, lighting conditions fluctuate, leading to poor-quality images and videos that subsequently affect the accuracy of image-based analyses. Various methodologies have been proposed to enhance visualization in low-light scenarios. Previous studies have explored non-uniform illumination models (2) to assess the contribution of illumination in segmented scenes. Additionally, convolutional neural networks (CNNs) have emerged as powerful mathematical models, employing multiple layers to autonomously identify crucial features within image data without manual intervention (3). Recent advancements in deep learning have furthered our understanding of CNNs and their applications in low-light image processing for object detection. Advanced CNN architectures now incorporate numerous layers, with higher levels contributing to increased output resolution (4-6). Moreover, the implementation of residual networks (ResNets) has revolutionized the training process by introducing fast connections that exploit both high-level and low-level features to bypass missing training layers (7). These ResNets offer efficient object recognition in challenging lighting conditions, providing a methodological advantage over traditional deep neural networks (8). Recent studies have emphasized the need to address low-light conditions efficiently for robust target recognition. Switching between low and high-resolution images is essential, and the integration of CNN models is pivotal in this pursuit (9). Additionally, contemporary approaches emphasize brightness enhancement and noise reduction through size-dependent subspace analysis techniques.

(Received 19th October 2023; Accepted 01st January 2024; Published 30th January 2024)

Object detection in low-light environments

Due to insufficient lighting, the recorded image information has many dark areas and noise (10,11). Images in dim lighting must be optimized to achieve precise target detection. In the process of using methods to improve low-light images, there are the following drawbacks:

- It requires complex structures and a large number of parameters.
- It requires more layers and more calculations.
- Training requires relevant data sets, but it isn't easy to obtain relevant images.

These problems make object detection systems less efficient and use more computing power (12). Adaptive truncation schemes can be used in size-dependent subspaces to remove noise (13). Deep Network methods (14) and traditional illumination and optimization methods (15) are also used to reduce noise. Recessed lighting can be combined with modified reflectors. It is used to improve images in dark environments (16, 17). Another night vision detector (NVD) approach is based on hierarchical features and contextual matching networks. Different lighting profiles can be designed independently of each other, although they overlap during the training phase (18). The training datasets are used, and the model uses a simple face-to-face global network. Another method is based on the Retinex multiscale discrete wavelet transform (19). It is generated by a CNN with channels and a Gaussian kernel to implement image enhancement and noise reduction networks. This architecture learns to insert images from pairs of dark and light ideas.

Object detection using gaussian distribution

Noise seriously affects the relationship between neighbouring pixels (20, 21). Functional differences between modified and unmodified regions can be identified using a set of Gaussian models to remove background information (22). Another classic technique is the algorithm (23), which combines the image-related Network (24). Provides the best noise reduction built into Fusion Net. Bayesian solutions evaluate ideal and unseen Gaussian backgrounds in the trained Network (25). Because it uses a Gaussian algorithm, shape changes can be approximated efficiently. The MG method (26) can model customarily distributed data to represent deep features. Converting representations from large datasets (such as ImageNet) to smaller datasets is just as effective. Existing Gaussian mixture models (GMMs) allow background subtraction strongly influenced by noise and dynamic backgrounds (27).

Object recognition by probabilistic method

According to this approach, survival can be assessed using a combination of femoral cartilage volume and peripheral magnetic resonance imaging (MRI). Magnification (EM) techniques are commonly used to simulate brain imaging. These methods also require unique noise reduction methods for each level (28). Another approach (29) extends from probabilistic atlases that provide information about healthy tissues to latent atlases that offer information about lesions. This general probabilistic model and its discriminant extension give the model semantic meaning. The author (30) developed a new algorithm using random objects and background distribution to obtain more accurate segmentation results. The proposed framework maximizes. Probabilistic models can be applied to various imaging colourimetry and magnetic resonance imaging. Before processing remotely captured images, the cloud content must be cleared. It is based on a combination of attention and probabilistic sampling mechanisms. Algorithm-centric correlations between spatially scaled multispectral images and spectral sections. Obtaining updated labels with multiple labels using fully convolutional networks (31) and choosing the appropriate sampling mode are crucial for high-quality image reconstruction (32). Sampling methods based on probabilistic quality functions can automatically adjust the sampling rate based on previously measured data. Constant random quality function. The incremental sampling technique avoids sampling delay.

Object detection using background subtraction methods

The rest of the background is essential to distinguish between stationary and moving objects. Dynamically changing contexts complicate the process and lead to erroneous results. Therefore, the Dynamic Moving Average (ARMA) model (33) uses the spatial-temporal correlations

between the input images to build a good background image model. The adaptive least squares method can be used to update dynamic soil properties. The blur map uses the C-fuzzy background subtraction method, which refers to the Fuzzy Cluster Neighborhood (FCFN) (34), to describe the temporal properties of pixels. Overcome ranking challenges by organizing everything on the backend and front end. Hyperspectral images (HSI) contain many bands and must be reduced in size before processing. Use the curvature filter to remove the noise and use the remaining background to get the first result. Specific shape layers can be used in adaptive weighting methods to achieve final quality. Fast and slow lighting changes also affect the background less mode. An adaptive local mean texture function (35) was introduced to solve this problem. Calculating adaptive thresholds for foreground pixels. Compare the background pattern with the sequence of video frames using the ALMT function on the foreground pixels. Choosing the proper background reduction method and related settings is crucial to achieving optimal object recognition in low-light conditions. The authors (36) studied several parameters of the background subtraction algorithm with the necessary parameters to detect the appearance of darkness.

Object detection using graph based network

Advances in image processing. According to the filters used, GCNNs can be divided into two categories: spatial techniques and spectral techniques. The lack of graphic guidance greatly hinders the learning process. Directed graph convolutional networks built with fast local convolution operators scale well to large graphs. Information about feature boundaries may be lost in high object detection video samples. The architecture works within the GCN framework and provides a mechanism for efficiently clustering shared super pixels. The author (36) proposed a new module of interest for super pixel encryption. Finally, adjustments are made through cognitive optimization to ensure consistency between essential factors. It can lead to the loss of information about shared features over long distances. The authors proposed a dense combination of multiscale CNN maps to increase the local contextual knowledge of the joints (37). Space and thoughtful units allow development. The nature of space and time. Each model layer has an independent kernel size, which leads to very flexible programming. Some changes are needed to improve image efficiency while addressing interference issues. [Graphic convolutional layers 3 to 6] can be added to the design of trainable neural networks, which helps to find the hidden features in the Network, thus improving the learning capabilities. Internet sustainability. The advantage of incorporating graph warping into existing CNNs is the flexibility to compute adjacency graphs, build compound object weights in non-local filters, and avoid operations. Indicates a predetermined amount. The non-cognitive basis elements can be used to solve the knowledge base integrity problem (38). The transformation-based knowledge graph model uses these parameter values to translate the knowledge base completion task.

Methodology

M-Resnet architecture

The M-ResNet architecture tackles the challenges of object detection in low-light conditions. It incorporates a selective search algorithm, replacing the sliding window approach to mitigate redundancy and reduce algorithmic complexity. This alteration enhances the algorithm's efficiency. Additionally, handcrafted feature extraction methods are substituted with a CNN. This CNN efficiently extracts features and improves the network's resilience to interference. Utilizing a pre-trained CNN model, such as AlexNet trained on ImageNet, extracts features to predict the presence of the target within the image frame or determine the class of the detected object. While the R-CNN model has significantly enhanced object detection performance, certain limitations persist. The M-ResNet architecture is augmented by additional layers to enhance image quality by mitigating low-light effects and delays, thereby improving object detection accuracy. The new layer operations include two-sided adaptive sampling and symmetric local binary sampling, as illustrated in Figure 1. These operations facilitate noise reduction while preserving edge details, allowing for precise object identification within video images. Low-light images serve as input in the initial stage, exhibiting reduced accuracy compared to typical images.

Figure 1: M-Resnet Architecture with New Layer Operations for Improved Object Detection and Low-Light Elimination

AIIE algorithm

To address the challenges of low-light images, the Adaptive Image Information Enhancement (AIIE) algorithm is implemented. This algorithm employs bilateral filtering, adaptive filtering, and symmetric local binary path computations to increase image brightness and enhance object detection accuracy for low-light images, as depicted in Figure 2.

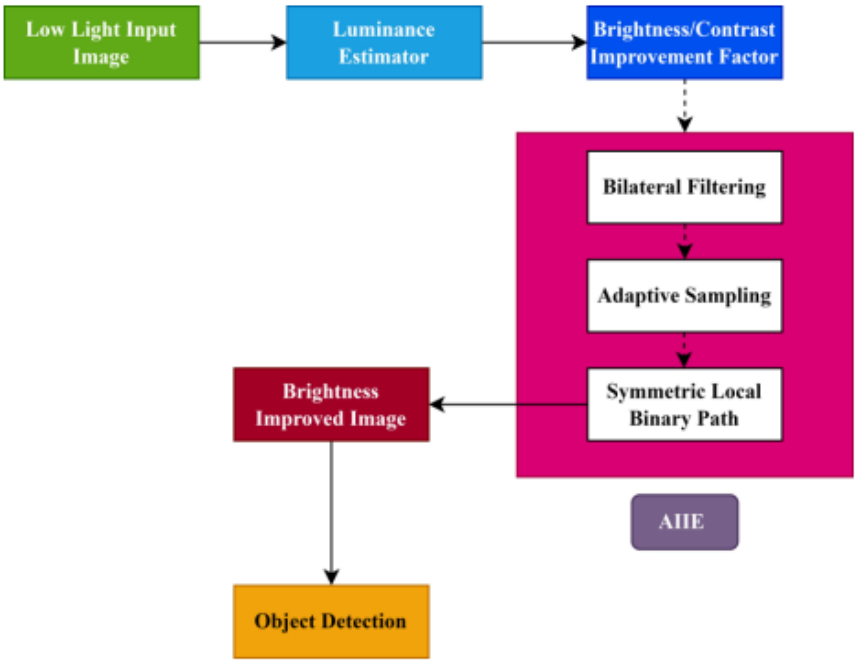

Figure 2: Adaptive Image Enhancement System Architecture

Bilateral filtering

The input image is processed by a non-linear binary filtering technique using the video sequence as a source. This method improves image smoothness while preserving edge information. BF Represents the bilateral filtering, and P and Q represent the weight of two images. It is shown in equation 1

$$-BFI_P = \frac{1}{W_P}\sum_{q\in S} G\sigma s\left(\|p-q\|\right) \quad G\sigma s\left(\|I_P - I_q\|\right) I_q \text{ ---------[1]}$$

$$\text{Space weight} \qquad \text{Range weight}$$

Pixel-weighted averaging is another name for this two-sided process, as the picture shows in Figure 3. It provides detailed information about the input image, which is helpful during processing. The Bilateral filtering is shown in equation 2 and 3. Noise cancellation process.

$$BilateralFiltering\left[I_{in}\right]_p = \frac{1}{W_p}\sum_{x_i\in\Omega} I(y_i) H_r\left(\|I(y_i)-I(y)\|\right) f_s\left(\|y_i - y\|\right) \text{----------[2]}$$

$$W_p = \sum_{x_i\in\Omega} H_r\left(\|I(y_i)-I(y)\|\right) f_s\left(\|y_i - y\|\right) \text{----------[3]}$$

Binary filtering combines field filters with area filters. It measures the average similarity and neighbours of a pixel and replaces it. In order to apply this proposed work to a CCTV system, sample images under suitable lighting conditions will be purchased beforehand. During observation, especially at night, the recommendation system compares the current image with the pictures taken from the imaged samples in a specific period. Exact components can be sample images superimposed on significant components of the existing image frame to allow the object recognition process to continue.

Adaptive sampling

The result of two-sided operations may contain pixel edges that cause aliasing effects in the image data. Streaks occur because curves and lines extend endlessly. Each pixel is displayed multiple times. A specific point (x, y) within an image pixel. The radiation density L can be calculated as follows in equation 4 and 5

$$L = \int_A^n p(x,y) f(x,y) dxdy \text{ ----------[4]}$$

$$X_i,\ i = 1,2,\ldots\ldots,n \text{ ----------[5]}$$

No additional sampling is required at any time. Therefore, adaptive sampling only up samples the pixels at the object's edge, thus preserving the object's edge in the equation 6.

$$L = \frac{1}{n}\sum_i^n X_i \text{ ----------[6]}$$

Symmetric local binary path

By determining the neighbourhood of each pixel and processing the result as a binary number. LBP operators in CCTV applications may notice changes in light changes. LBP encoded pixel value. The LPB can be calculated by determining the difference between the pixel intensities of adjacent pixels in equations 7 and 8. In, where n denotes the location of the adjacent pixel. It represents the size of n, which is 8. If adjacent pixels have equal or greater values, set the value to 1; otherwise, set it to zero.

$$LBP = \sum_{i=0}^{p-1} s\left(n_i - G_C\right) 2^i \text{ ----------[7]}$$

$$s(x) = \begin{cases} 1 \ , if \ \ x > 0 \\ 0, \ otherwise \end{cases} \text{----------[8]}$$

Results

Dataset

To illustrate the difference between various low-light images in CCTV systems, additional images from three different datasets from Plants, Animals, and Birds were selected for the test. The diverse dataset contained images captured under different low-light conditions, including severely low, moderately low, and normally lit scenarios. Test results are compared with current methods. During the training phase, 6452 images were used in the dataset. The algorithm was trained using a subset of the dataset that covered a spectrum of low-light conditions, ensuring diversity in illumination levels for robust model training. Validation of the algorithm's performance was carried out on a distinct subset of images to gauge its ability to detect objects accurately across various low-light conditions. In Figure 3, three different images

represent the low-light conditions of the new existing gate and the architecture of the modified new gate. In the coconut group, two variants of the same image can be saved for testing, as shown in Figure 3. The input image is pre-processed under normal lighting conditions (Figure 5). The photo has good lighting conditions are selected.

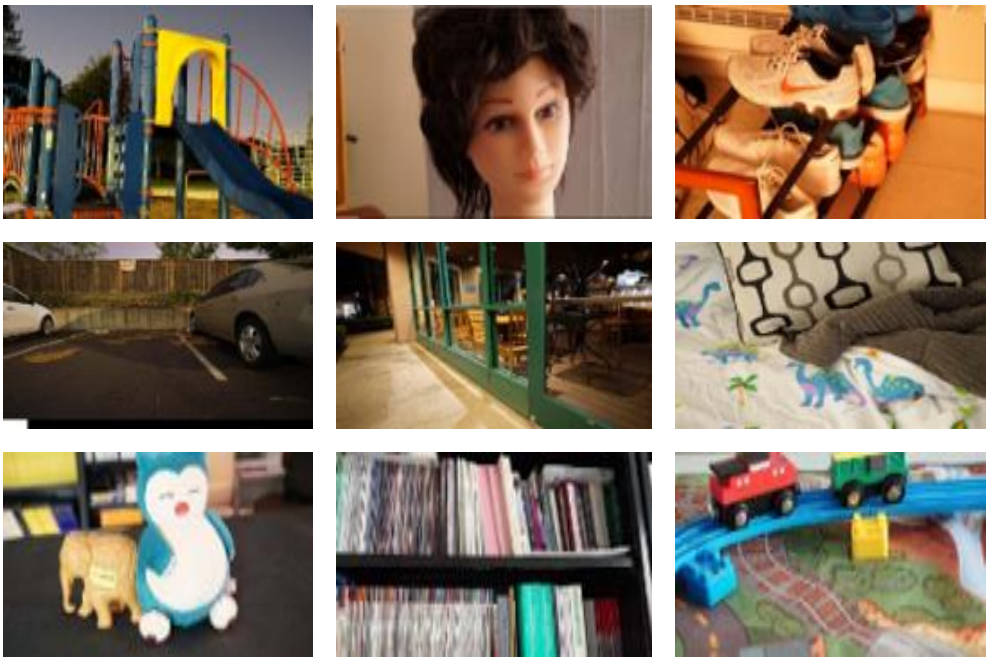

Figure 3: Sample images from the dataset used.

Analysis

Precision, Recall, and F1-score calculations were performed for each illumination level, providing insights into the algorithm's capability to detect objects accurately under varying low-light conditions. A zebra is selected, and the probabilities of all three creatures appearing are 99.9, 99.8, and 99., respectively. A similar image can be seen in Fig 4(a): Low Light Input Image and Fig 4(b): Brightness Improved Image. The second image, now tested with the resnet model, shows four individual zebras. Poor lighting conditions can cause this false output. Fig 4(c) Accuracy in Low Light and Fig 4(d): Accuracy in Brightness Improved Image.

Figure 4(a): Low Light Input Image

Figure 4(b): Brightness Improved Image

Figure 4(c): Accuracy in Low Light

Figure 4(d): Accuracy in Brightness Improved Image

Table 1 shows the accuracy comparison between the low-light and bright-light images. The Accuracy for low light is 74%, and for high light, it should be 96%. Figure 5 represents the Accuracy of object detection in various luminance parameters.

Several parameters from the coco, Wild Track, and CIFAR datasets can be used to evaluate performance, including recall, precision, F1 score, pixel resolution, fusible crosshair, and fusible crosshair. Recall provides the integrity of predictions drawn from the ground truth. Accuracy demonstrates the relationship between positive findings and ground truth. It provides the rate of overlap between the target output and the expected output. The average IoU metric is measured as the average of all value intersections associated with the semantic layer. Various ML techniques are evaluated, and their performance metrics are estimated to define the malicious RDP sessions.

$$Accuracy = \frac{TP+TN}{Total\ subjects} \times 100\% \quad [9]$$

$$Precision = \frac{TP}{TP+FP} \times 100\% \quad [10]$$

$$F1\ score = 2 \times \frac{TP}{TP+FN} \quad [11]$$

$$Sensitivity/Recall = \frac{TP}{TP+FN} \times 100\% \quad [12]$$

$$AP\ score = \sum_n (Recall_n - Recall_{n-1}) \times Precision \quad [13]$$

$$Sepcificity = \frac{TN}{FP+TN} \times 100\% \quad [14]$$

$$GMeean = \sqrt{Sensitivity + Specificity} \quad [15]$$

TP is a True Positive, TN is a True Negative, FP is a False Positive, and FN is a False Negative value.

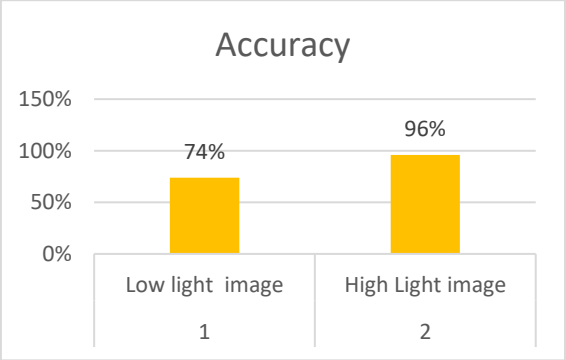

Figure 5: Accuracy in object detection

This tabulation compares the various algorithm parameters with AIIE (Adaptive Image Information Enhancement Algorithm) algorithms to find the precision, accuracy, recall, and f1 score. The various algorithms used for comparison are the ACNN, Faster R-CNN, Gaussian mixture, and DCGAN models. A comparison of different Algorithms is shown in Table 2.

Table 1: Image Type

S. No.	Input Image Type	Accuracy
1	Low light image	74%
2	High Light image	96%

Fig 6 shows the overall performance of the Adaptive Image Information Enhancement Algorithm. The experimental values indicate that the AIIE algorithms give more precision when compared to other algorithms. For example, the Precision of AIIE, ACNN model, Faster R-CNN, Gaussian mixture model, and DCGAN model are 78,63,55,70.68 respectively.

Fig 7 shows the overall Recall performance of the Adaptive Image Information Enhancement Algorithm. The experimental values indicate that the AIIE algorithms give more precision when compared to other algorithms. For example, the Recall of AIIE, ACNN model, Faster R-CNN, Gaussian mixture model, and DCGAN model are 84,85,78,81,81 respectively.

Figure 8 shows the overall F1 Score performance of the Adaptive Image Information Enhancement Algorithm. The experimental values indicate that the AIIE algorithms give more precision when compared to other algorithms. For example, the F1 Score of AIIE, ACNN model, Faster R-CNN, Gaussian mixture model, and DCGAN model are 84,71,70,71,74, respectively.

Figure 9 shows the overall Pixel Accuracy performance of the Adaptive Image Information Enhancement Algorithm. The experimental values show that the AIIE algorithms give more precision when compared to other algorithms. For example, the Pixel accuracy of AIIE, ACNN model, Faster CNN, Gaussian mixture model, and DCGAN model are 95,87,74,87,92, respectively.

Discussion

The proposed system employing the AIIE algorithm represents a significant advancement in improving object detection accuracy under low-light conditions. Its strengths lie in its ability to enhance image quality, thereby facilitating more accurate object detection compared to existing systems. By utilizing the AIIE algorithm, this system effectively

The AIIE algorithm's superiority becomes evident in the comparative analysis against existing models. It consistently outperforms these models

in critical metrics such as precision, recall, F1 score, and pixel accuracy. Visual representations further emphasize the algorithm's excellence, providing a clear understanding of its superior performance compared to other evaluated models. However, despite its significant strengths, the system does present limitations. One notable concern is its potential computational complexity, which might require substantial resources. Additionally, real-time implementation in scenarios necessitating immediate object detection and response might pose a challenge due to computational demands.

Moreover, while the system displays proficiency across various datasets, its performance in more diverse environmental conditions or with different object types might vary. Generalizing its success beyond the specific datasets used in this evaluation remains an area for further exploration. Despite these limitations, the AIIE-based system presents a compelling solution for addressing low-light image challenges in object detection tasks. Its consistent performance enhancements and robustness across diverse datasets signify its potential in applications reliant on accurate object detection under varying lighting conditions, such as surveillance and security systems. Continued research and refinement could further amplify its applicability and performance in real-world scenarios.

Table 2: Comparison of various algorithm

S. No.	Method	Precision	Recall	F1-score	Pixel accuracy
1	AIIE Algorithm	78	86	84	95
2	ACNN model	63	85	71	87
3	Faster R-CNN	55	78	70	74
4	Gaussian mixture model	70	81	71	79
5	DCGAN model	68	81	74	82

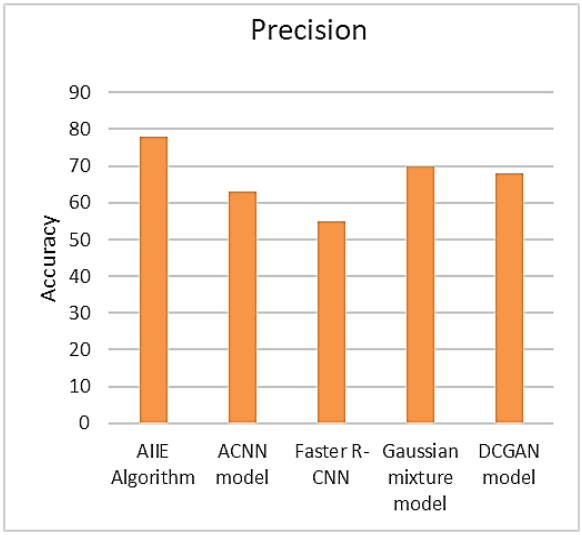

Figure 6: Precision comparison of the existing and proposed algorithms

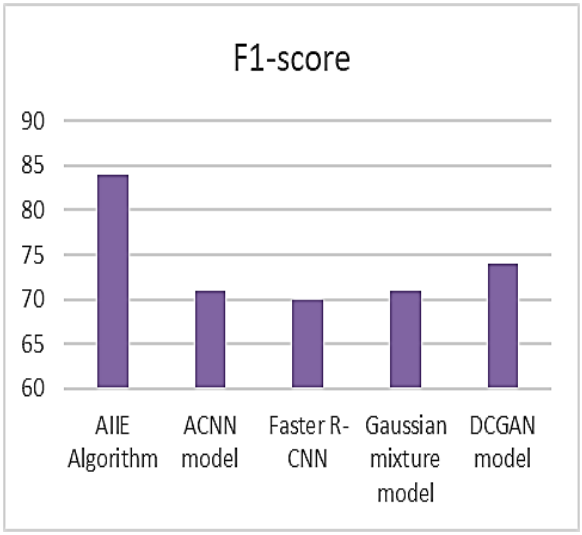

Figure 7: Recall comparison of the existing and proposed algorithms

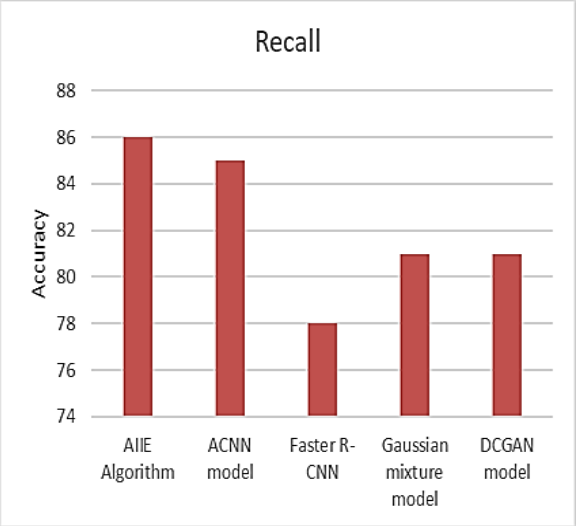

Figure 8: F1 score comparison of the existing and proposed algorithms

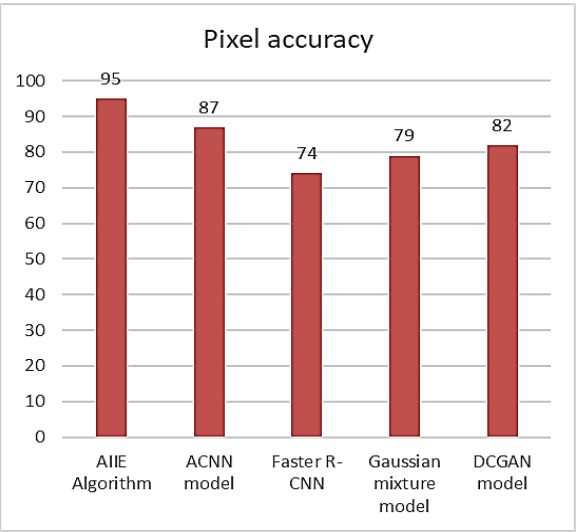

Figure 9: Pixel comparison of the existing and proposed algorithms

Conclusion

This paper presents AIIE, an integrated component within an enhanced ResNet architecture, addressing
object detection challenges in low-light CCTV systems. The ResNet model incorporates connection hops, mitigating issues with fading gradients during training. The inclusion of the ellipse layer significantly bolsters low-light imaging capabilities without compromising performance. Operations within this layer, such as employing binary filters for enhanced lighting conditions, adaptive sampling to avoid anti-aliasing, and utilizing local binary models, offer more precise image details. These processes enable deeper image analysis, enhancing object detection accuracy. Extensive evaluations across varied datasets consistently demonstrate AIIE's superiority over existing methods in handling low-light conditions in CCTV object detection. However, increased computational time in processing excessively low luminance images remains a limitation. The AIIE integrated ResNet model signifies a substantial leap in low-light object detection for CCTV systems. Its promise lies in improved accuracy, opening avenues for advancements in real-time surveillance applications. This innovation lays the groundwork for future developments in addressing illumination challenges in object detection systems. Future research aims to innovate light data enhancement methods without relying on distinct light conditions, striving to further improve performance and processing speeds in object detection workflows.

Abbreviations

Nil

Acknowledgments

The authors would like to acknowledge all the faculties of their respective institutions for their help during the study and especially thank the heads of both departments for their moral support.

Author contributions

The authors confirm sole responsibility for the following: study conception and design, data collection, analysis and interpretation of results, and manuscript preparation.

Conflict of interest

None

Ethics approval

This research paper does not necessitate ethics approval as it does not involve human subjects, sensitive data, or experiments on animals.

Funding for the study

Nil

References

1. Patrikar DR, Parate MR. Anomaly detection using edge computing in a video surveillance system. International Journal of Multimedia Information Retrieval. 2022 Jun;11(2):85-110.doi: 10.1007/s13735-022-00227-8.
2. Sun L, Jeon B, Soomro BN, Zheng Y, Wu Z, et al. Fast superpixel-based subspace low-rank learning method for hyperspectral denoising. IEEE Access. 2018;6(1):12031–12043.doi:10.1109/ACCESS. 2018. 2808474.
3. Lv Q, Feng W, Quan Y, Dauphin G, Gao L, et al. Enhanced-random-feature-subspace-based ensemble CNN for the imbalanced hyperspectral image classification. IEEE Journal of Selected Topics in Applied Earth Observations and Remote Sensing. 2021;14(1):3988–3999. doi: 10.1109/JSTARS.2021. 3069013.
4. Li C, Qin X, Xu X, Yang D, Wei G. Scalable graph convolutional networks with fast localized spectral filter for directed graphs. IEEE Access. 2020;8(1):105634–105644. doi: 10.1109/ACCESS. 2020.2999520.
5. Su H, Jung C. Perceptual enhancement of low-light images based on two-step noise suppression. IEEE Access.2018;6(1):7005–7018.doi: 10.1109/ACCESS. 2018.2790433.
6. Guo Y, Lu Y, Liu RW, Yang M, Chui KT. Low-light image enhancement with regularized illumination optimization and deep noise suppression. IEEE Access.2020;8(1):145297–145315. doi: 10.1109/ ACCESS.2020.3015217.
7. Xiao Y, Jiang A, Ye J, Wang MW. Making of night vision: Object detection under low-illumination. IEEE Access.2020;8(1):123075–123086.doi:10.1109/ ACCESS. 2020.3007610.
8. Chen G, Li L, Jin W, Li S. High-dynamic range, night vision, image-fusion algorithm based on a decomposition convolution neural network. IEEE Access. 2019;7(1):169762–169772. doi: 10.1109/ ACCESS.2019.2954912.
9. Jiang Y, Gong X, Liu D, Cheng Y, Fang C, et al. EnlightenGAN: Deep light enhancement without paired supervision. IEEE Transactions on Image Processing. 2021;30(1):2340–2349. doi: 10.1109/ TIP.2021.3051462.
10. Guo Y, Ke X, Ma J, Zhang J. A pipeline neural network for low-light image enhancement. IEEE Access. 2019;7(1):13737–13744. doi: 10.1109/ACCESS. 2019.2891957.
11. Xue D, Lei T, Jia X, Wang X, Chen T, et al. Unsupervised change detection using multiscale and multiresolution Gaussian-mixture-model guided by saliency enhancement. IEEE Journal of Selected Topics in Applied Earth Observations and Remote Sensing. 2020;14(1):1796–1809. doi: 10.1109/ JSTARS.2020.3046838.
12. Han L, Li X, Dong Y. Convolutional edge constraint-based U-net for salient object detection. IEEE Access. 2019;7(1):48890–48900. doi: 10.1109/ACCESS. 2019.2910572.
13. Riaz F, Rehman S, Ajmal M, Hafiz R, Hassan A, et al. Gaussian mixture model based probabilistic modeling of images for medical image segmentation. IEEE Access. 2020;8(1):16846–16856. doi10.1109/ ACCESS.2020.2967676.
14. Ghimpeţeanu G, Batard T, Bertalmío M, Levine S. A decomposition framework for image denoising algorithms. IEEE Transactions on Image Processing. 2016;25(1):388–399. doi:10.1109/TIP.2015. 2498413.
15. Helou ME, Susstrunk S. Blind universal Bayesian image denoising with Gaussian noise level learning. IEEE Transactions on Image Processing. 2020;29(1):4885–4897. doi: 10.1109/TIP.2020. 2976814.
16. Luthi M, Gerig T, Jud C, Vetter T. Gaussian process morphable models. IEEE Transactions on Pattern Analysis and Machine Intelligence. 2017;40 (8):1860–1873. doi: 10.1109/TPAMI.2017.2739743.
17. Rippel O, Mertens P, Konig E, Merhof D. Gaussian anomaly detection by modeling the distribution of normal data in pre-trained deep features. IEEE Transactions on Instrumentation and Measurement. 2021;70(1):1–13. doi: 10.1109/TIM.2021.3098381.
18. Antico M, Sasazawa F, Takeda Y, Jaiprakash AT, Wille ML, et al. Bayesian CNN for segmentation uncertainty inference on 4D ultrasound images of the femoral cartilage for guidance in robotic knee arthroscopy. IEEE Access. 2020;8(1):223961–223975. doi: 10.1109/ACCESS.2020.3044355.
19. Wang K, Liu MZ. Object recognition at night scene based on DCGAN and faster R-CNN. IEEE Access. 2020;8(1):193168–193182. doi: 10.1109/ACCESS. 2020.3032981.
20. Kim T, Lee J, Choe Y. Bayesian optimization-based global optimal rank selection for compression of convolutional neural networks. IEEE Access. 2020;7(1):17605–17618. doi:10.1109/ACCESS.2020.2968357.
21. Menze BH, Leemput KV, Lashkari D, Riklin-Raviv T, Geremia E, et al. A generative probabilistic model and discriminative extensions for brain lesion segmentation—with application to tumor and stroke. IEEE Transactions on Medical Imaging. 2015;35(4):933–946.doi:10.1109/TMI.2015.2502596.
22. Zhang Y, Zheng W, Leng K, Li H. Background subtraction using an adaptive local median texture feature in illumination changes urban traffic scenes. IEEE Access. 2020;8(1):130367–130378. doi: 10.1109/ACCESS.2020.3009104.
23. Iqbal E, Niaz A, Memon AA, Asim U, Choi KN. Saliency-driven active contour model for image segmentation. IEEE Access. 2020;8(1):208978–208991. doi: 10.1109/ACCESS.2020.3038945.
24. Shao Z, Zhou W, Deng X, Zhang M, Cheng Q. Multilabel remote sensing image retrieval based on fully convolutional network. IEEE Journal of Selected Topics in Applied Earth Observations and Remote Sensing. 2020;13(1):318–328. doi:10.1109/JSTARS. 2019.2961634.
25. Grosche S, Koller M, Seiler J, Kaup A. Dynamic image sampling using a novel variance-based probability mass function. IEEE Transactions on

Computational Imaging.2020;6(1):1440–1450.doi:10.1109/TCI. 2020.3031077.
26. Li J, Pan ZM, Zhang ZH, Zhang H. Dynamic ARMA-based background subtraction for moving objects detection. IEEE Access. 2019;7(1):128659–128668. doi:10.1109/ACCESS.2019.2939672.
27. Yu T, Yang J, Lu W. Dynamic background subtraction using histograms based on fuzzy c-means clustering and fuzzy nearness degree. IEEE Access. 2019;7(1):14671–14679.doi:10.1109/ACCESS. 2019.2893771.
28. Xiang P, Song J, Qin H, Tan W, Li H, et al. Visual attention and background subtraction with adaptive weight for hyperspectral anomaly detection. IEEE Journal of Selected Topics in Applied Earth Observations and Remote Sensing. 2270–2283.doi:10.1109/JSTARS. 2021. 3052968.
29. Kim T, Lee J, Choe Y. Bayesian optimization-based global optimal rank selection for compression of convolutional neural networks. IEEE Access. 2020;7(1):17605–17618. doi:10.1109/ACCESS.2020.2968357.
30. Menze BH, Leemput KV, Lashkari D, Riklin-Raviv T, Geremia E, et al. A generative probabilistic model and discriminative extensions for brain lesion segmentation—with application to tumor and stroke. IEEE Transactions on Medical Imaging. 2015;35(4):933–946.doi:10.1109/TMI.2015. 2502596.
31. Zhang Y, Zheng W, Leng K, Li H. Background subtraction using an adaptive local median texture feature in illumination changes urban traffic scenes. IEEE Access. 2020;8(1):130367–130378. doi: 10.1109/ACCESS.2020.3009104.
32. Iqbal E, Niaz A, Memon AA, Asim U, Choi KN. Saliency-driven active contour model for image segmentation. IEEE Access. 2020;8(1):208978–208991. doi:10.1109/ACCESS.2020.3038945.
33. Shao Z, Zhou W, Deng X, Zhang M, Cheng Q. Multilabel remote sensing image retrieval based on fully convolutional network. IEEE J Sel Top Appl Earth Obs Remote Sens. 2020;13(1):318–328. doi:10.1109/ JSTARS.2019.2961634.
34. Grosche S, Koller M, Seiler J, Kaup A. Dynamic image sampling using a novel variance-based probability mass function. IEEE Trans Comput Imaging. 2020;6(1):1440–1450. doi:10.1109/TCI.2020. 3031077.
35. Li J, Pan ZM, Zhang ZH, Zhang H. Dynamic ARMA-based background subtraction for moving objects detection. IEEE Access. 2019;7(1):128659–128668. doi:10.1109/ACCESS.2019.2939672.
36. Yu T, Yang J, Lu W. Dynamic background subtraction using histograms based on fuzzy c-means clustering and fuzzy nearness degree. IEEE Access. 2019;7(1):14671–14679. doi:10.1109/ACCESS. 2019.2893771.
37. Xiang P, Song J, Qin H, Tan W, Li H, et al. Visual attention and background subtraction with adaptive weight for hyperspectral anomaly detection. IEEE J Sel Top Appl Earth Obs Remote Sens. 2021;14(1):2270–2283. doi:10.1109/JSTARS.2021. 3052968.
38. Karthik K, Shanmugapriya N. Design and Implementation of Multi-Retinal Disease Classification Using Deep Neural Network. In: Proceedings of the 2023 Eighth International Conference on Science Technology Engineering and Mathematics (ICONSTEM); 2023. p. 1-6. doi:10.1109/ICONSTEM56934.2023.10142864.